The impact of bonded interactions on the ground-state geometries of a small flexible polymer

Tomas Koci[1], Kai Qi[1] and Michael Bachmann[1,2,3]

[1] Soft Matter Systems Research Group, Center for Simulational Physics, The University of Georgia, Athens, Georgia 30602, USA
[2] Instituto de Física, Universidade Federal de Mato Grosso, 78060-900 Cuiabá (MT), Brazil
[3] Departamento de Física, Universidade Federal de Minas Gerais, 31270-901 Belo Horizonte (MG), Brazil

E-mail: koci@smsyslab.org, qi@smsyslab.org, bachmann@smsyslab.org
Homepage: http://www.smsyslab.org

Abstract. Bonded interactions in coarse-grained models of elastic polymers are commonly represented by the finitely extensible nonlinear elastic (FENE) potential. In this study, we perform parallel multicanonical Monte Carlo simulations to examine the impact of an additional Lennard-Jones term in the bonded potential on the geometry of ground-state structures of a short polymer. Employing microcanonical inflection point analysis and conformational analysis, we construct a hyper-phase diagram and identify ground-state structures with two distinct geometries.

1. Introduction

The physical and chemical functionality of biopolymers and synthetic variants is intimately related to their conformational structure. Therefore, the systematic study of their dynamic and structural properties is of a fundamental importance and a major topic of current interdisciplinary research. Theoretical approaches are generally not adequate due to the prohibitive complexity of even the simplest molecular systems [1]. On the other hand, computational methods such as the replica-exchange [2], multicanonical [3, 4], and Wang-Landau sampling [5], have proven to be most effective. Despite the vast increase in the availability of computational resources over the past decade, simulations of fully atomistic models remain a major challenge. Hence a clever choice of suitable coarse-grained models with a reduced number of parameters is often a prerequisite to a successful computational study. In this paper, we consider a generic model of the flexible elastic homopolymer and examine the effects of adding an extra Lennard-Jones term to the bonded potential. The unexpected consequences for the ground-state structures highlight the importance of a careful choice of model parameters.

2. Model and Methods

We employ a generic model of a flexible elastic homopolymer to study the effects of the shape and width of the bonded potential on the formation of low-energy structures for a polymer chain with $N = 15$ monomers. Finite-size effects are essential and the 15mer shows a particularly distinct and clear transition behavior, which makes it a perfect candidate for this systematic study.


Content from this work may be used under the terms of the Creative Commons Attribution 3.0 licence. Any further distribution of this work must maintain attribution to the author(s) and the title of the work, journal citation and DOI.
Published under licence by IOP Publishing Ltd

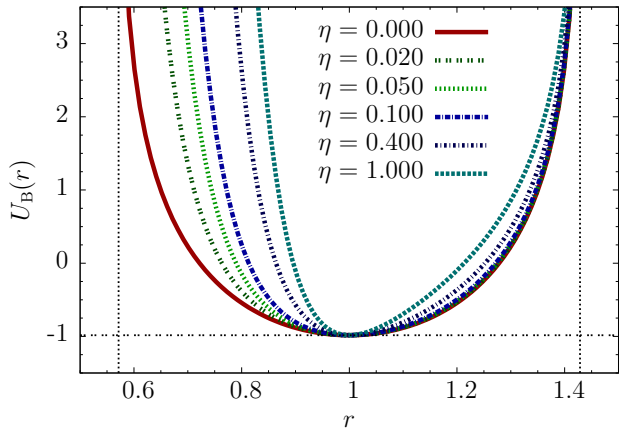


Figure 1. The modified bonded potential $U_{\mathrm{B}}(r)$, modeled by the FENE and LJ interactions. The strength of the Lennard-Jones term is controlled by the bond flexibility parameter $\eta \in [0, 1]$.

Non-bonded interactions are represented by the truncated and shifted Lennard-Jones (LJ) potential

$$U_{\mathrm{LJ}}^{\mathrm{trunc}}(r_{ij}) = \begin{cases} U_{\mathrm{LJ}}(r_{ij}) - U_{\mathrm{LJ}}(r_c), & \text{if } r_{ij} \leq r_c, \\ 0, & \text{if } r_{ij} > r_c, \end{cases} \tag{1}$$

where

$$U_{\mathrm{LJ}}(r) = 4\epsilon \left[\left(\frac{\sigma}{r}\right)^{12} - \left(\frac{\sigma}{r}\right)^{6} \right]. \tag{2}$$

The energy scale is set to $\epsilon = 1$ and the van-der-Waals radius to $\sigma = r_0/2^{1/6}$, where $r_0 = 1.0$ is the location of the potential minimum. We select a cut-off radius at $r_c = 2.5\,\sigma$ and introduce a shift $U_{\mathrm{LJ}}(r_c) \approx -0.0163169\,\epsilon$ to avoid discontinuities in the potential. In our model, monomers adjacent in the linear chain interact via a modified bonded potential

$$U_{\mathrm{B}}(r) = -\frac{1}{2} K R^2 \ln \left[1 - \left(\frac{r - r_0}{R} \right)^2 \right] + \eta(U_{\mathrm{LJ}}(r) + \epsilon) - (\epsilon + U_{\mathrm{shift}}), \tag{3}$$

where $R = 3/7$ and $K = 98/5$. In addition to the standard anharmonic FENE (finitely extensible nonlinear elastic) potential [6, 7, 8], the modified potential contains an additional Lennard-Jones term adjusted by a bond flexibility control parameter η. The bonded potential is shifted by $-(\epsilon + U_{\mathrm{shift}})$ in order to match the minimum energy with the non-bonded interactions.

The maximum bond extension is limited by the FENE potential, which diverges as $r \to r_0 \pm R$. Increasing the value of η introduces asymmetry to the bonded potential and the energy cost associated with non-optimal bond lengths is increased. In particular, compressed bonds result in high energy penalties as η becomes large. The effects of different η values on the shape and width of the bonded potential is exhibited in Fig. 1. The total energy of a configuration $\mathbf{X} = (\vec{r}_1, ..., \vec{r}_N)$ with the monomer-monomer distances $r_{ij} = |\vec{r}_i - \vec{r}_j|$ is given by

$$E(\mathbf{X}) = \sum_{i<j}^{N} U_{\mathrm{LJ}}(r_{ij}) + \sum_{i=1}^{N-1} U_{\mathrm{B}}(r_{i\,i+1}). \tag{4}$$

In order to enhance the sampling of low-energy configurations, a parallel version of multicanonical sampling [3, 4, 9] is employed in this simulation. The standard multicanonical runs are performed in K replicas independently with the same initial weight functions but different random seeds. Displacement updates are proposed within a cubic box of edge lengths $d = 0.3r_0$ and accepted according to the probability

$$P(X \to X') = \min[1, W(E(X'))/W(E(X))], \tag{5}$$

where $W(E(X))$ represents the weight function of a given configuration X. After the ith iteration, since the weights are identical in each thread, the energy histograms obtained for each replica can simply be summed up:

$$H^i(E) = \sum_{k=1}^{K} H_k^i(E). \tag{6}$$

The total histograms are combined with the current weights to calculate the weights for the subsequent iteration by utilizing the error-weighted recursive scheme [1, 3, 4].

To construct the hyper-phase diagram, we use the generalized microcanonical inflection-point analysis [1, 10]. This approach has the advantage of uniquely and systematically locating the transition energies and thus is commonly employed to study pseudophase transitions in finite-size systems. By applying the principle of minimal sensitivity [11] to the derivatives of microcanonical entropy $S(E)$, the $(2n+1)$th-order transition (n is a positive integer) is identified from the least sensitive inflection point of the $2n$th-derivative of entropy and the positive valley in the $(2n+1)$th-derivative curve. For a $2n$th-order transition, the least sensitive inflection point in the $(2n-1)$th-derivative of entropy together with the negative peak in the $2n$th-order derivative curve are utilized to locate the transition energy. The specialty of the first-order-like transition is that it can be distinguished from the back-bending region in the inverse temperature $\beta(E) \equiv T^{-1}(E) = dS(E)/dE$ and the corresponding positive peak in the $\gamma(E) = d\beta(E)/dE$ curve.

3. Results

3.1. Canonical and microcanonical analysis

First we discuss the results of canonical statistical analysis applied to our generic model. Heat-capacity curves as functions of temperature (Fig. 2(a)) are constructed using the time series of data collected in the multicanonical production run. At $T \approx 0.34$, broad prominent peaks, indicating the freezing transition, are identified for all simulated η values. At this transition, globular structures change to more compact crystalline or amorphous structures. For $\eta = 0$, an additional peak emerges at $T = 0.11$, suggesting the existence of a solid-solid transition. With increasing values of η the peak becomes more pronounced as it gradually shifts towards zero temperature and finally disappears when $\eta \geq 0.1$. However, the order of the individual transitions remains ambiguous and the broad peaks of the freezing transition may envelope several transitions which cannot be resolved by the methods of canonical analysis. Therefore we further examine the system using a more systematic and robust approach. One such method that has proven to reliably signal transitions is the microcanonical inflection-point analysis [10].

The microcanonical results are shown in Fig. 2(b-d) for six different values of η. Careful inspection of the first and second derivatives of $\beta(E)$ in the energy region $E \in [-45.5, -33]$ reveals that the broad peak in the canonical specific heat encloses two distinct transition signals; clear indication that the freezing transition is a two-step process. The first signal located at $E \approx -44$, is a fourth-order transition indicated by the corresponding least sensitive inflection point in $\delta(E)$. The second transition, found at $E \approx -38$, is of third order for $\eta \leq 0.2$, but it is classified as a second-order transition for higher values of the bond flexibility control parameter. In agreement with the canonical results, we have also identified signals corresponding to a solid-solid transition for values of $\eta \leq 0.1$. For $\eta = 0.02$ and 0.05, the negative-valued peaks in $\gamma(E)$ at energies $E = -49.7$ and -50.4 respectively, indicate a second-order transition. The inflection point in $\gamma(E)$ and the corresponding positive valley in $\delta(E) = d\gamma(E)/dE$ at $E = -48.92$ reveal that for $\eta = 0.00$ the solid-solid transition is of third order.

The hyper-phase diagram is constructed on the basis of the signals identified in the microcanonical analysis and plotted in Fig. 3. In the "gas" pseudophase at high energies, the

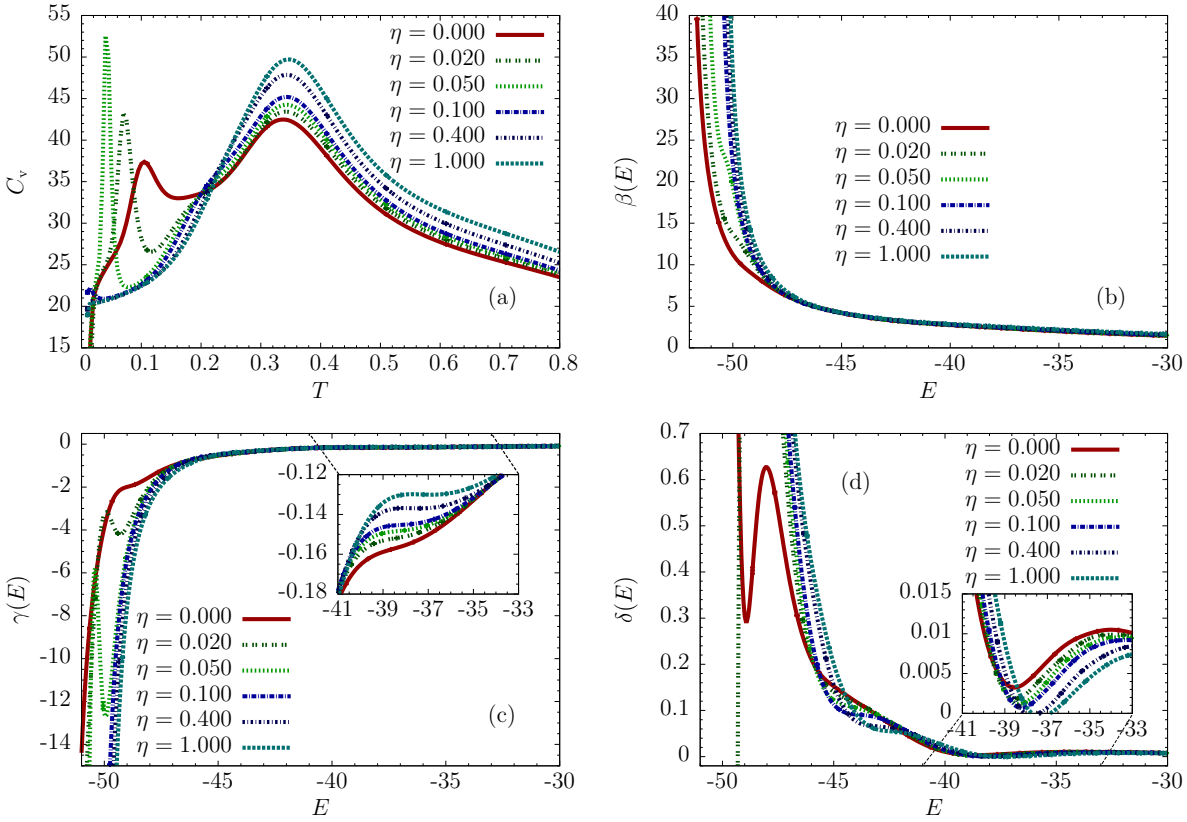


Figure 2. (a) Heat capacity $C_{\rm v}$, (b) microcanonical inverse temperature $\beta(E)$, and (c,d) its first and second derivatives $\gamma(E)$ and $\delta(E)$, respectively.

polymer expands in free space and forms random-coil structures. As the energy decreases, the expanded chain undergoes a second-order collapse transition and enters the "liquid" pseudophase consisting mainly of globular structures. Passing the third/second-order transition associated with the nucleation process, the polymer enters the $S_{\rm ic}$ pseudophase in which incomplete icosahedral structures become dominant. Further decrease in energy weakens thermal fluctuations and allows for the formation of a stable surface layer. The transition associated with the surface formation process is of fourth order. Visual inspection of low-energy structures reveals that icosahedral geometries are dominant. However, for $\eta \leq 0.1$, the additional solid-solid transition suggests the existence of low-energy conformations with unexpected geometric properties. In order to examine the low-energy structures systematically, we carry out a careful structural analysis utilizing a suitable set of order parameters.

3.2. Structural analysis

Various order parameters, such as the number of monomer-monomer contacts, radius of gyration, or radial and angular distributions, have proven to provide valuable insight into the thermodynamic and structural properties of polymer systems. Based on the microcanonical results in Fig. 3, we expect the existence of two solid phases when the strength of the bond flexibility parameter is sufficiently small ($\eta \leq 0.1$). We aim to identify the dominant structures in the low-energy phases and to gather additional data supporting the existence of the solid-solid transition line. For this purpose, we employ a set of order parameters exploiting the symmetry

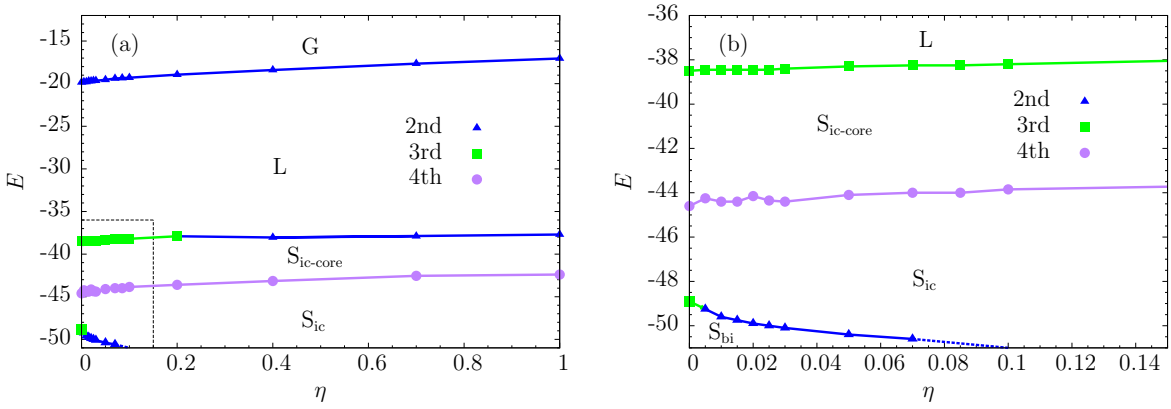


Figure 3. (a) Microcanonical hyper-phase diagram parameterized by energy and the bond flexibility control parameter η. Here, G, L, and S stand for "gas", "liquid", and "solid" structural phases, respectively. The $S_{\mathrm{ic-core}}$ pseudophase consists mostly of incomplete icosahedral structures. S_{ic} and S_{bi} incorporate compact icosahedral and bihexagonal structures, respectively. (b) Enlarged section detailing the low energy region for $\eta < 0.15$. The solid-solid transition line is extended by a dashed empirical line constructed based on the data provided by structural analysis.

properties of real spherical harmonics [12].

We define a polymer core to consist of monomers within a distance $r_{\mathrm{core}} < 1.25\sigma$ of the central monomer, which has been chosen to be nearest to the center of mass. Let $\mathcal{C} = \{\vec{r}_1, ..., \vec{r}_M\}$ be the coordinates of a core with M monomers. Various core geometries can be distinguished using the set of rotationally invariant order parameters

$$Q_l = \left[\frac{4\pi}{2l+1} \sum_{m=-l}^{l} |\rho_{l,m}|^2 \right]^{1/2}, \tag{7}$$

where

$$\rho_{l,m} = \frac{1}{M} \sum_{i=0}^{M} \mathrm{Y}_{l,m}(\vec{r}_i) \tag{8}$$

is the average of the real spherical harmonics evaluated at the locations of the core monomers. The connection between the real and complex spherical harmonics is given by

$$\mathrm{Y}_{lm} = \begin{cases} \frac{i}{\sqrt{2}} \left[\mathrm{Y}_l^m - (-1)^m \mathrm{Y}_l^{-m} \right] & \text{if} \quad m < 0, \\ \mathrm{Y}_l^m & \text{if} \quad m = 0, \\ \frac{1}{\sqrt{2}} \left[\mathrm{Y}_l^{-m} + (-1)^m \mathrm{Y}_l^m \right] & \text{if} \quad m > 0. \end{cases} \tag{9}$$

Using of the order of 10^6 polymer structures per value of η, we computed Q_l up to $l = 6$ and found that Q_6 can be used most effectively to resolve the geometries of the low-energy conformations. We present the results in the form of intensity plots in Fig. 4. The probability of detecting a structure with a specific value of the order parameter at an energy E is represented by shading; red indicating the maximum probability and black corresponding to zero. In agreement with the microcanonical and canonical results, we detect a single solid phase for $\eta > 0.1$, corresponding to

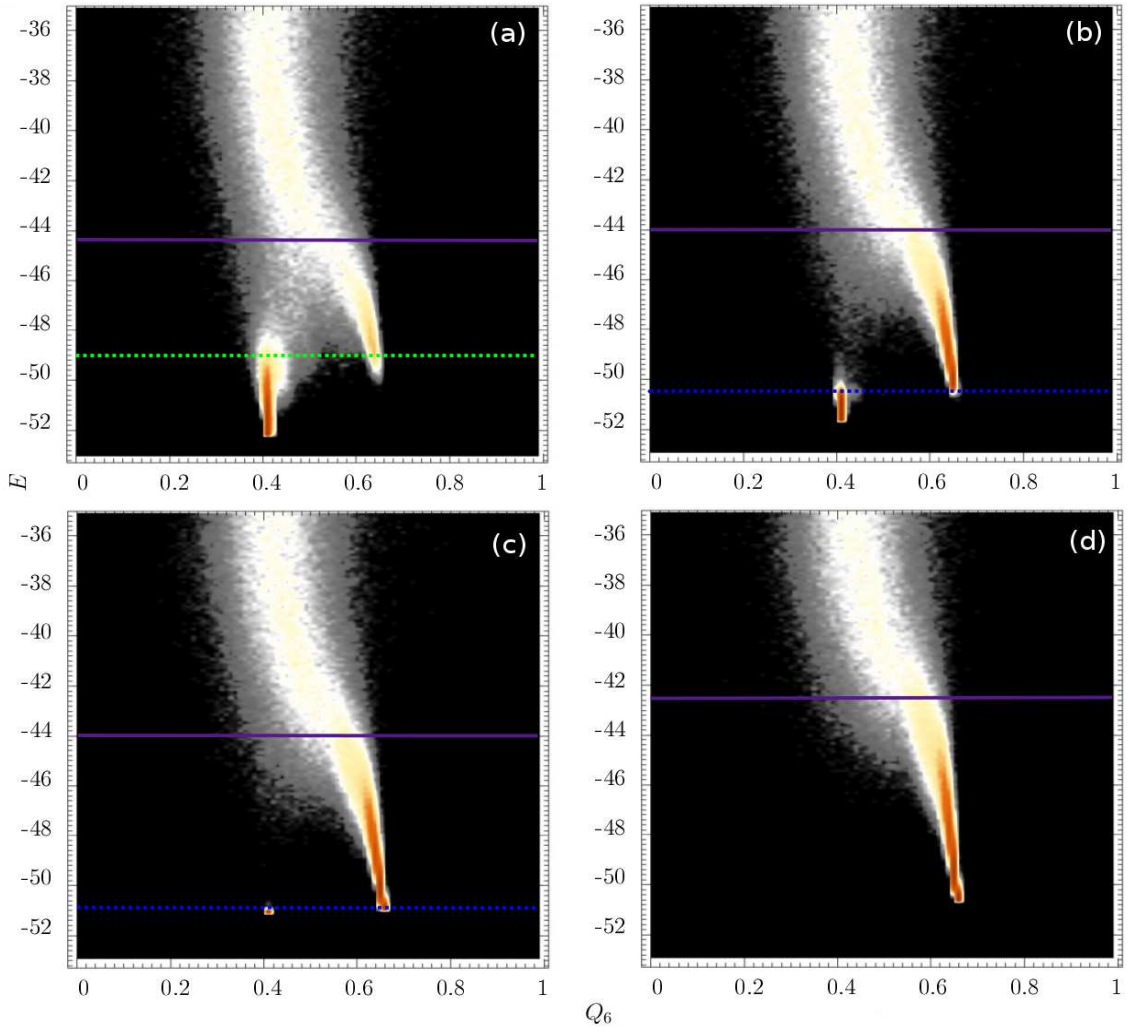


Figure 4. (a,b,c,d) Intensity plots of the Q_6 order parameter for a 15mer with $\eta = 0.00, 0.05, 0.10, 1.0$. The shading indicates the probability of detecting a configuration with a given value of the order parameter, red being the maximum probability and black being the lowest. The freezing and the solid-solid transitions are indicated by solid and dashed horizontal lines respectively. For $\eta \leq 0.1$, the polymer has two distinct solid phases. In addition to the icosahedral phase ($Q_6 \approx 0.65$) the polymer is found in the bihexagonal phase at low energies ($Q_6 \approx 0.41$).

the narrow funnel in Q_6 below the transition line at $E \approx -43$. The dominant structures in this region contain an icosahedral core which is typically found in the ground-state conformations of many short polymer chains. Below $\eta = 0.1$, the 15mer explores an additional solid phase, as indicated by the appearance of a second funnel centered around $Q_6 \approx 0.41$. Structures which populate this phase possess an unusual bihexagonal geometry which has also been recently found in longer chains. The energy at which both phases coexist agrees well with the microcanonical estimates for the solid-solid transition. Representative structures of both solid phases are shown in Fig. 5.

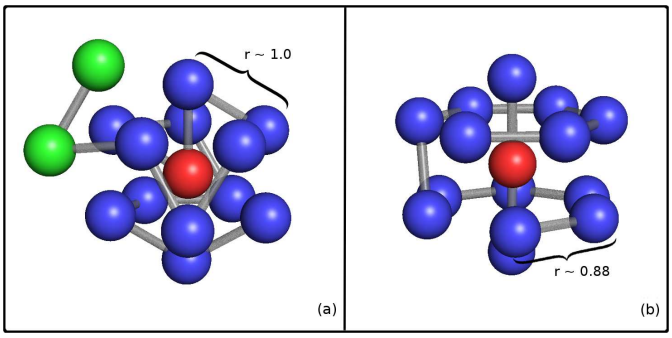


Figure 5. Two distinct low-energy structures of the elastic 15-mer. (a) Compact structure with a stable icosahedral core and two monomers displaced onto the incomplete second layer. (b) The bihexagon is the preferred ground-state geometry for $\eta \leq 0.1$.

The shape of the bonded potential has undoubtedly a strong effect on the geometry of the ground state. Having identified the two dominant structure types, we may ask why the additional LJ term in the bonded potential eventually precludes the existence of the bihexagonal phase. The answer is readily obtained by comparing the average bond lengths for the icosahedral and bihexagonal structures. The bihexagon accommodates all monomers into a single shell allowing for a larger number of non-bonded interactions and consequently lower energy. However, the two six-monomer rings of the bihexagon contain significantly compressed bonds ($r_{\mathrm{bond}} \approx 0.88 r_0$), which become energetically infeasible as η increases. In contrast, we find near-optimal bond lengths in the icosahedron ($r_{\mathrm{bond}} \approx r_0$), hence the "narrowing" of the bonded potential imposes no additional energetic penalty.

4. Summary

By means of multicanonical simulations of a generic model for elastic, flexible polymers, we have investigated the structural behavior of a 15-mer upon changing a model parameter η that controls the shape of the bonded potential. For small values of this parameter, a freezing transition into an icosahedral phase precedes a solid-solid transition into low-energy states with bihexagonal geometry. The non-optimal bond lengths found in bihexagonal conformations cause a large energy penalty due to the "narrowing" of the bonded potential if η is increased. Hence only a single solid phase remains for $\eta > 0.1$, which is icosahedral. The striking consequences of a relatively small modification to the standard model of elastic, flexible homopolymers illustrate the importance of a careful choice of model parameters.

References

[1] Bachmann M 2014 *Thermodynamics and Statistical Mechanics of Macromolecular Systems* (Cambridge: Cambridge University Press)
[2] Hukushima K and Nemoto K 1996 *J. Phys. Soc. Jpn.* **65** 1604
[3] Berg B A and Neuhaus T 1991 *Phys. Lett.* B **267** 249
[4] Janke W 1998 *Physica* A **254** 164
[5] Wang F and Landau D P 2001 *Phys. Rev. Lett.* **86** 2050
[6] Bird R B, Curtiss C F, Armstrong R C and Hassager O 1987 *Dynamics of Polymeric Liquids* 2nd ed. (New York: Wiley)
[7] Kremer K, Grest G S, 1990 *J. Chem. Phys.* **92** 5057
[8] Milchev A, Bhattacharya A, Binder K 2001 *Macromolecules* **34** 1881
[9] Zierenberg J, Marenz M and Janke W 2013 *Comp. Phys. Comm.* **184** 1155
[10] Schnabel S, Seaton D T,Landau D P and Bachmann M 2011 *Phys. Rev.* E **84** 011127
[11] Stevenson P M 1981 *Phys. Rev.* D **23** 2916
[12] Neirotti J P, Calvo F, Freeman D L and Doll J D 2000 *J. Chem. Phys.* **112** 10340